KINETIC VERSUS HYDRODYNAMIC SOLAR WIND MODELS*: by J. LEMAIRE

Institut d'Aéronomie Spatiale de Belgique, 3, Avenue Circulaire,
B- 1180 Brussels, Belgium

Résumé : Les principales approximations hydrodynamiques des équations générales de transport sont présentées avec leurs limites de validité. Il est montré que ces approximations ne sont applicables à l'étude du vent solaire que jusqu'à une distance radiale de 5 à 10 rayons solaires. Au-delà de cette distance, dans l'exosphère ionique du Soleil, des approximations cinétiques sont préconisées. Un exemple de modèle cinétique (exosphérique) du vent solaire est discuté. Bien qu'un certain nombre de moments calculés dans ce modèle cinétique correspondent aux valeurs observées à 1 UA, le désaccord constaté pour l'anisotropie de la température nous suggère de considérer des modèles cinétiques plus élaborés où l'effet des collisions Coulombiennes serait traité comme une correction du premier ordre de la fonction de distribution des vitesses.

Introduction. Alternative points of view and lively controversies are met in Physics, as well as in other human activities. Indeed from the fields of Quantum Mechanics to Cosmology there is quite a number of well known controversies which have focused interest of a wide audience upon certain crucial scientific questions. The opposition between the proponents of hydrodynamic solar wind models and kinetic solar wind models is just one more example which is still alive in our memories so that it is unnecessary to recall more historical details. Nearly two decade after the rise of this controversy we have tried to reconsider in a different perspective the two alternative points of view, emphasizing the complementary more than the contradictory aspects of both theoretical approaches.

The Hydrodynamic approximations. Let us first recall how the hydrodynamic approximations are derived from the general Boltzmann equation which describes the evolution of the particle velocity distribution function, $f(\vec{c},t)$. Taking velocity moments of Boltzmann's equation, a straightforward procedure determines an infinite set of Moments Equations of which the five first are the transport equations governing the density (zero order moment), the components of the bulk velocity (first order moment), and the temperature (a second order moment) of a neutral or ionized gas.

The equation governing the bulk velocity contains components of the pressure or stress tensors. The equation governing second order moments contains third order moments, etc.. There are a number of approaches to limiting the number of Moments Equations, and to obtaining a closed set of differential equations which can then be integrated for given boundary conditions.

In fig. 1 different approaches leading to different hydrodynamic approximations are listed. A very comprehensive discussion of all these hydrodynamic approximations has been given by Schunk (1977) and should not be repeated here. An impressive number of solar wind models are based on these different hydrodynamic approximations. A comparative analysis of the various hydrodynamic solutions has been given by Hundhausen (1972).

Limitations of the hydrodynamic approximations. Although it is unnecessary to repeat a detailed analysis of the limitations of hydrodynamic approximations, however, it is worth recalling here that the Euler, Navier-Stokes, or Burnett approximations of the general transport equations have been established exclusively for collision-dominated gases : i.e. when the interaction force between particles is well determined, and, when the velocity distribution is not too far from the maxwellian equilibrium function as the result of collisions.

The latter condition implies, for steady state flow regimes, that the mean free path (m.f.p.) of the interacting particles is small with respect to D, the dimension of the system. In the solar wind the characteristic dimension of the system is the density scale height :

$$H = \left| \frac{d\ell n\ n}{dr} \right|^{-1} , \qquad (1)$$

The curve 2 in figure 2 shows the value of the scale height (H) derived from an observed coronal electron density distribution (n_e) which is given by the curve 1.

For a fully ionized gas the collision mean free path to be considered is that given by Spitzer (1956) for binary Coulomb interactions. The angular deflections mean free path of a thermal proton in the solar corona and in the solar wind is approximately given (in km) by

$$(\ell_D)_p = 0.072 \frac{T_p^{\ 2}}{n_p} \qquad (2)$$

where T_p and n_p are the proton temperature (°K) and density (cm^{-3}), respectively.

For the plasma density illustrated by curve 1 in figure 2, the proton mean free path can be determined as a function of the radial distance (r) or as a function of height (h) above the solar limb. The larger the proton temperature (T_p), the larger the m.f.p. and the smaller is the exobase altitude (h_o) where $(\ell_D)_p$ equals the density scale height (H). This is shown by the dashed curve 3 in figure 2 giving the altitudes of the proton exobase for a continuous set of proton temperatures ranging between $T_p = 5 \times 10^5$K and $T_p = 2 \times 10^6$K. The dashed curve 4 in figure 2

gives the exobase altitude for the thermal electrons as a function of the electron temperature $T_e(h_o)$.

Above these altitudes in the solar corona, Coulomb collisions with impact parameters smaller than the Debye length are infrequent and they play a secondary role only in the evolution of the velocity distribution function. In this region of the solar atmosphere, called the ion-exosphere, the m.f.p. is larger than the scale height, and the hydrodynamic approximations deduced from Chapman-Enskog's or Grad's approaches are difficult to justify. Indeed these particular approximations of the most general transport equations are based on the assumption that the Knudsen Number (ℓ/D) is much smaller than unity. Obviously this is not the case in the ion-exosphere i.e. above an altitude of 6.3 Sun radii when $T_p = 9 \times 10^5$K and $T_e = 1.4 \times 10^6$K (Lemaire and Scherer, 1971a, 1973).

Below the exobase altitude, only, can a hydrodynamic approximation confidently be used to determine the density, bulk velocity and temperature distributions in the solar corona. Although the general Moments Equations must be satisfied everywhere (even in the ion-exosphere), the hydrodynamic approximations depending on special closing procedures of these Moments Equations, however, are questionable under certain physical conditions like those in the distant solar wind plasma. Even when the velocity distribution happens to be close to a maxwellian (i.e. with relatively small first order correction terms) in a Knudsen gas (i.e. when $\ell/H > 1$), can an hydrodynamic approximation not be justified; for instance, in a Knudsen gas, the heat flow cannot be assumed proportional to the temperature gradient (Shizgal, 1977).

The possibility to replace particle collisions by wave-particle interactions has sometimes been invoked to justifying the relevance of the hydrodynamic approximations beyond the exobase altitude. This would

imply for wave-particle interactions to have similar effects on the velocity distribution as Coulomb collisions. Furthermore, assuming the Navier-Stokes approximation is applicable to a collisionless plasma when wave-particle interactions are important, would imply that the stress tensor and heat flow can still be expressed in terms of the lower order moments of the velocity distribution function as for a gas dominated by particle collisions (i.e. stress tensor being determined by velocity shears; the heat flow being proportional to the gradient of the gas temperature) ! Furthermore, even if these assumptions could be proven, eventually, to be correct for certain types of wave-particle interactions it remains to be demonstrated that the proportionality factors (i.e. the viscosity coefficients; the thermal conductivity coefficient) have still the usually infered $T^{5/2}$ temperature dependence as for Coulomb interactions. Therefore, some reservations must be made when the conductivity and viscosity coefficients are simply modified by an ad-hoc factor to account for wave-particle interactions in hydrodynamic solar wind models.

Hydrodynamic solar wind models. The first hydrodynamic solar wind model was based on Euler approximation, assuming an isotropic pressure tensor and isothermal temperature distribution (Parker, 1958). Later on, Navier-Stokes equations were extensively used to model the solar wind expansion. This mathematical improvement did not change drastically the density and bulk flow distribution in the corona itself (i.e. within 4 - 6 solar radii) where the application of the hydrodynamic approximations is not questionnable. The discrepancies between hydrodynamic models generally appear at larger radial distances (for instance at 1 AU). Therefore we can limit the following discussion to the most simple expansion model of the solar corona: i.e. the isothermal model.

Figures 3 and 4 are distributions of bulk velocities (w) and plasma densities (n) for five hydrodynamic models. The temperature of the electrons and protons are both assumed to be 10^6K. At the reference altitude

h_{ref} = 0.5 Sun radius, the electron and proton densities are equal to 10^7 cm^{-3}; this is a value taken from Pottash (1960). These boundary conditions which are in the range of observed values, are identical for all models considered in figures 3 and 4. However, the bulk velocity at the reference level is different in each case. The curve c corresponds to the well known critical solution of the Euler hydrodynamic equations. ($w_{ref:}$ = 3.996 km/sec at the reference level). The curves a and b represent subcritical (or subsonic) solutions of the hydrodynamic equations; the curves d and e correspond to Parker's supercritical solutions. For these latter models the density (n) as well as the scale height (H, defined by eq. 1) drop rapidly to zero at an altitude below the "critical point". The "critical point" is illustrated by a square dot in figures 3 and 4.

The distributions of mean free paths of thermal protons have been calculated by Brasseur and Lemaire (1977) for each of the five models. The solid curves in figures 3 and 4 correspond to the portion of the models where the mean free paths are smaller than the local scale heights. The dashed curves correspond to the extension of the hydrodynamic solutions in the collisionless region of the solar corona. The exobase for each model is indicated by a solid dot. The locus of exobase altitudes is illustrated by a dotted curve.

From these results it can be deduced that the exobase altitude (where the validity of hydrodynamic models break down) is generally below the "critical point" where the flow velocity becomes supersonic. The bulk velocity at the exobase (where the Knudsen number becomes equal to unity), is still smaller than the thermal velocity of the protons. Consequently, the critical point is located in the collisionless region of the solar corona (Brasseur and Lemaire, 1977). For the collisionless region Chamberlain (1960), Jockers (1970), Lemaire and Scherer (1971), Eviatar

and Schulz (1975) and others suggest using exospheric approaches i.e. kinetic approximations to model the solar wind expansion.

A kinetic solar wind model. When the polarisation electrostatic field distribution is determined to maintaining local quasi-neutrality and zero parallel electric currents in the coronal plasma, an exospheric theory of the solar wind expansion can account for the actual acceleration of positively charged particle to supersonic velocities at 1 AU.

A review of the early developments of kinetic solar wind models has been given by Lemaire and Scherer (1973). It is unnecessary to repeat these details, but it might be useful to recall the assumptions and limitations of kinetic models presently available.

Although the collision frequency is not strictly zero, it is considered that the particle trajectories are determined only by the gravitational field, electrostatic field and magnetic field distributions. The adiabatic moment is also supposed to be invariant. A convenient function, $F(\vec{c})$, of the particle velocities $(\vec{c})$ is then choosen at the exobase as a boundary condition for the collisionless Boltzmann-Vlasov equation. A linear combination of truncated Maxwellian distribution functions $\left(N_j \exp\left(-\frac{m(\vec{c} - \vec{U}_j)^2}{2kT_j}\right)\right)$ is usually taken. The parameters N_j, T_j and U_j characterising the displaced Maxwellians are adjusted to fit the actual density (n), temperature (T) and bulk speed (w) observed or calculated at the exobase altitude. Higher order moments of $F(\vec{c})$ can also be adjusted by adapting the parameters of $F(\vec{c})$ to fit the corresponding moments of the actual velocity distribution. Hence, in the exospheric models introduced by Lemaire and Scherer (1971a) there is no zero-order discontinuity for the lower order moments of the particle velocity distribution at the exobase.

Since any function of the constants of motion is a solution of the collisionless Boltzmann-Vlasov equation, the values of $F(\vec{c})$ and of its moments at any point in the exosphere can easily be obtained from their corresponding values at the exobase. Detailed analytical expressions of the lower order moments as a function of the gravitational and electric potential have been given by Lemaire and Scherer (1971b, 1972d) for different boundary conditions and different magnetic field geometries. Figure 5 shows the density, bulk velocity perpendicular temperature and average temperature in a kinetic solar wind model calculated by Lemaire and Scherer (1972b). The parameters N_j, U_j and T_j have been adjusted to obtain respectively $n_e = n_p = 3.1 \times 10^4$ cm^{-3}, $T_p = 9.84 \times 10^5$K, $T_e = 1.52 \times 10^6$K at the exobase, i.e. at the radial distance $r_o = 6.6$ solar radii. The densities, bulk velocities, and temperatures observed at 1 AU during quiet Solar Wind conditions range between the limits indicated by error bars in Figure 5.

The Quiet Solar Wind conditions (Hundhausen, 1970) are compared in Table 1 to the numerical results obtained for the kinetic model (LSb) of Lemaire and Scherer (1971a). The agreement between the observed and calculated values is satisfactory for quite a number of moments of the velocity distribution i.e. for the density (n_E), the bulk velocity (W_E), the particle flux (F_E), the average and perpendicular temperature of both electrons and protons ($\langle T \rangle$, $T_\perp$), the total kinetic energy flux (E_E), and for the heat conduction flux (C_E). However, in this kinetic model the temperature or pressure anisotropy at 1 AU is discordingly high compared to the observed values. This discrepancy cannot be explained by the already excessive temperature anisotropies at the exobase resulting from the boundary conditions adopted.

If the average solar wind temperatures can be predicted more or less correctly by collisionless model calculation, it must be admitted, however, that these models cannot account for the actual distribution of

TABLE 1 : Comparison of the Quiet Solar-Wind Conditions with the Results of the Kinetic Model LSb, which is a best fit solution to these Quiet Solar-Wind Conditions.

Conditions	Hundhausen [1970]	Kinetic Model LSb	Units
W_E	320	320	km sec^{-1}
n_E	5.4	7.18	cm^{-3}
F_E	1.73	2.30	10^8 cm^{-2} sec^{-1}
$< T_e >_E$	10 to 12 x 10^4	11.7 x 10^4	°K
$< T_p >_E$	4.8 10^4	4.8 x 10^4	°K
$(T_{\parallel}/T_{\perp})_e$	1.1 to 1.2	3.05	
$(T_{\parallel}/T_{\perp})_p$	3.4	164	
E_E	2.4 x 10^{-1}	2.0 x 10^{-1}	erg cm^{-2} sec^{-1}
C_{eE}	1 x 10^{-2}	5.1 x 10^{-2}	erg cm^{-2} sec^{-1}

temperature anisotropies for solar wind protons and electrons. Some pitch angle scattering mechanism must therefore be responsible for the reduction of the temperature anisotropy without affecting too much the average temperature : $\langle T \rangle = \frac{1}{3} (T_{\parallel} + 2T_{\perp})$. As suggested by Axford (1971, personal communication) the residual Coulomb collisions could contribute to produce the necessary reduction of $T_{\parallel} / T_{\perp}$ without changing $\langle T \rangle$. Indeed, the Coulomb collision time for angular deflections are much shorter than for energy equipartition. Consequently, the particle pitch angles can be changed more easily than the energy spectrum. It can therefore be concluded with Lemaire and Scherer (1971a), that Coulomb collisions could provide the wanted mechanism to reduce the temperature anisotropy below values predicted by an exospheric model calculation. The results of Leer and Axford (1972) also support this conclusion.

Conclusions : Even if less questionable than the hydrodynamic approximation, the kinetic or collisionless approximation does not lead to fully satisfactory models of the solar wind at large radial distances. Even if the effects of Coulomb collisions are small, when cumulated over a distance of several scale heights (H) they can account for a significant reduction of the temperature anisotropy, as observed at 1 AU. But improved kinetic approximations including the effects of Coulomb collisions as a first order correction are required to say more about the subject, and to evaluate how large are the residual discrepancies which should be explained by wave-particle interactions.

It can also be concluded that hydrodynamic and kinetic applications to the solar wind should be considered as complementary approaches, when applied within their own validity ranges : i.e. in the region close to the Sun for the hydrodynamic approximations, and beyond 5-10 Solar radii for the kinetic approaches.

References

BRASSEUR, G., and LEMAIRE, J., Planet. Sp. Sc., 25, 201, 1977.

BURNETT, D., Proc. Lond. Math. Soc., 39, 385, 1935.

CHAMBERLAIN, J.W., Astrophys. J. 131, 47, 1960.

CHAPMAN, S., Phil. Trans. Roy. Soc. A. 216, 279, 1916.

CHEW, G.F., GOLDBERGER, M.L. and LOW F.E., Proc. Roy. Soc. London, A, 236, 112, 1956.

EVIATAR, A. and SCHULZ, M., Astrophys. and Space Sc., 39, 65, 1976.

ENSKOG, D., Dissertation, Upsala, 1917.

GRAD, H., Comm. Pure and Appl. Math., 2, 331, 1949.

HUNDHAUSEN, A.J., Rev. Geophys. Space Phys., 8, 729, 1970.

HUNDHAUSEN, A.J., Coronal Expansion and Solar Wind, Springer, Berlin, 1972.

JOCKERS, K., Mitt. Astron. Ges., 25, 217, 1968.

JOCKERS, K., Astron. Astrophys., 6, 219, 1970.

LEER, E. and AXFORD, W.I., Solar Phys., 23, 238, 1972.

LEMAIRE, J. and SCHERER, M., J. Geophys. Research, 76, 7479, 1971a.

LEMAIRE, J. and SCHERER, M., Phys. Fluids, 14, 1683, 1971b.

LEMAIRE, J. and SCHERER, M., Phys. Fluids, 15, 760, 1972a.

LEMAIRE, J. and SCHERER, M., Bull. Cl. Sci. Acad. Roy. Belgique, 5s, t. LVIII, 1112, 1972b.

LEMAIRE, J. and SCHERER, M., Rev. Geophys. Space Physics, 11, 427, 1973.

MACMAHON, A., Phys. Fluids, 8, 1840, 1965.

PARKER, E.N., Astrophys. J., 128, 664, 1958.

POTTASCH, S.R., Astrophys. J., 131, 68, 1960.

SCHUNK, R.W., Rev. Geophys. Space Phys., 15, 429, 1977.

SHIZGAL, B., Planet. Space Sciences, 25, 203, 1977.

SPITZER, L.Jr., Physics of fully ionized gases, Interscience, New York, 1956.

SRIVASTAVA, M.P. and BHATNAGAR, P.L., Plasma Phys., 16, 79, 1974.

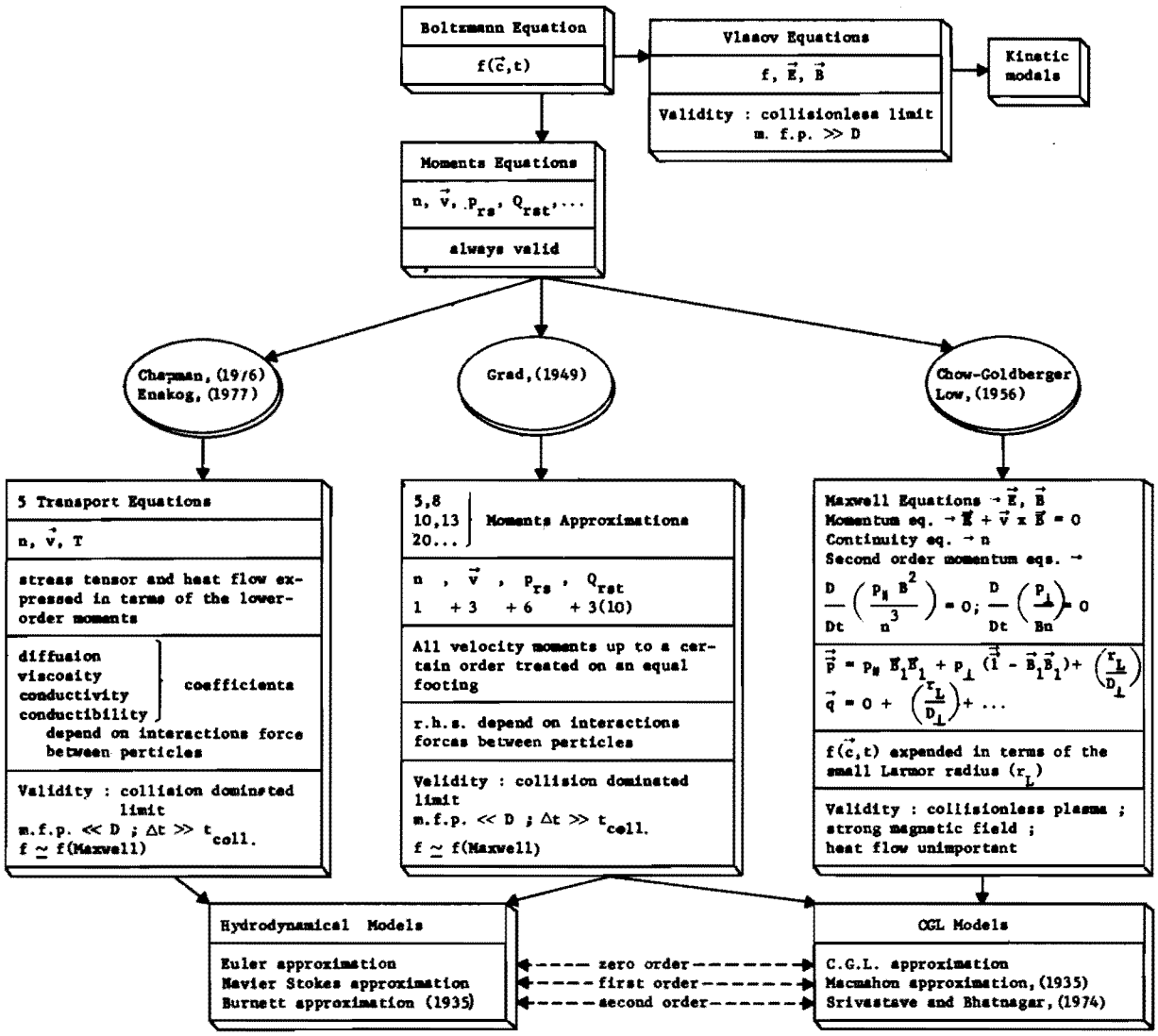

Fig. 1.- Table of hydrodynamic and kinetic approximations of the general transport equations.

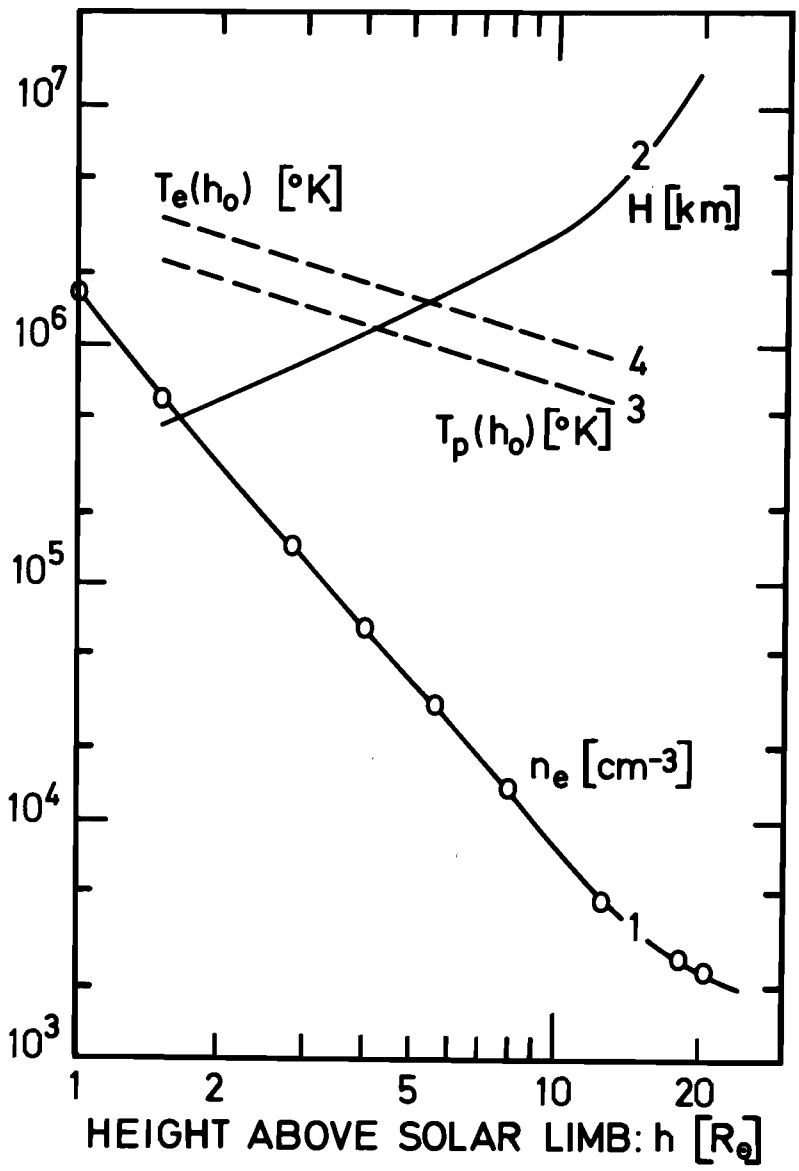

Fig. 2.- Curve 1 shows the equatorial electron number density distribution per cubic centimeter in the solar corona observed during an eclipse near minimum in the sunspot cycle as reported by *Pottasch* [1960]; curve 2 gives the corresponding density scale height H in kilometers; curves 3 and 4 illustrate, respectively, the proton and electron temperatures at the exobase altitude h_o expressed in solar radii.

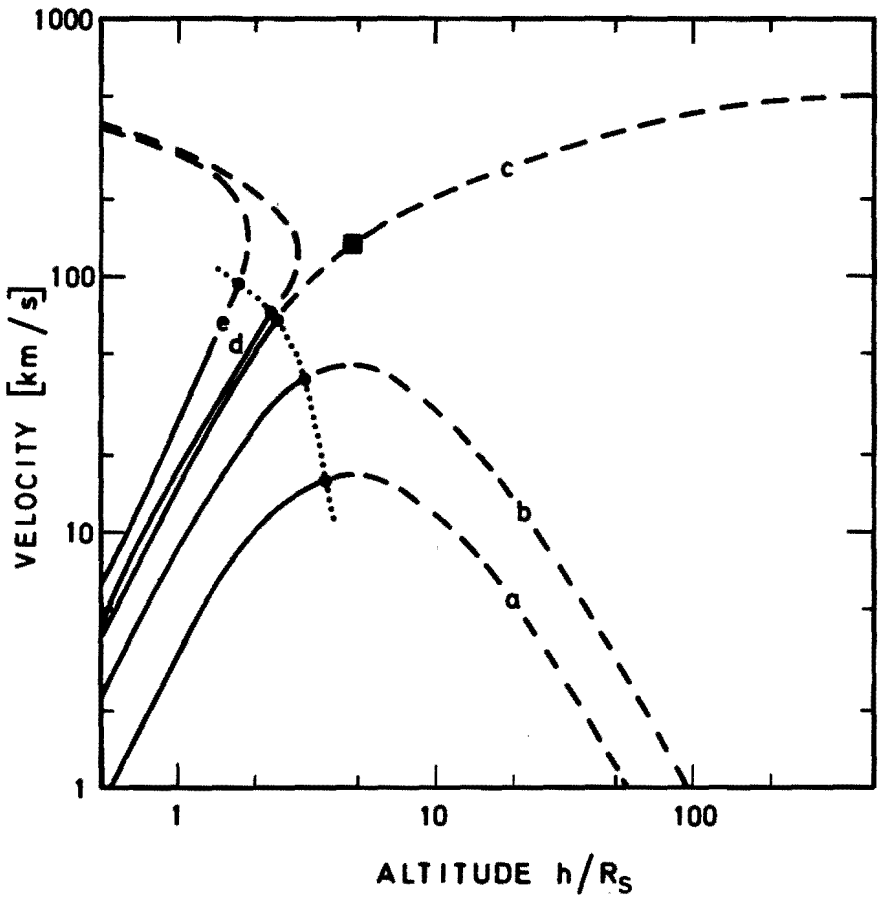

Fig. 3.- Solar wind flow velocities.
The solid and dashed curves refer to hydrodynamic isothermal models for which $T_e = T_p = 10^6$K; at $h_o = 0.5\ R_s$; (a) $w_o = 0.8$ km/s; (b) $w_o = 2.15$ km/s; (c) $w_o = (w_o)_c = 3.996$ km/s; (d) $w_o = 4.5$ km/s; (e) $w_o = 7.6$ km/s. The solid dots indicate for each of these five models the exobase altitude (h_{exb}) and flow speed (w_{exb}). The solid square corresponds to the critical point of the hydrodynamic Euler equations.

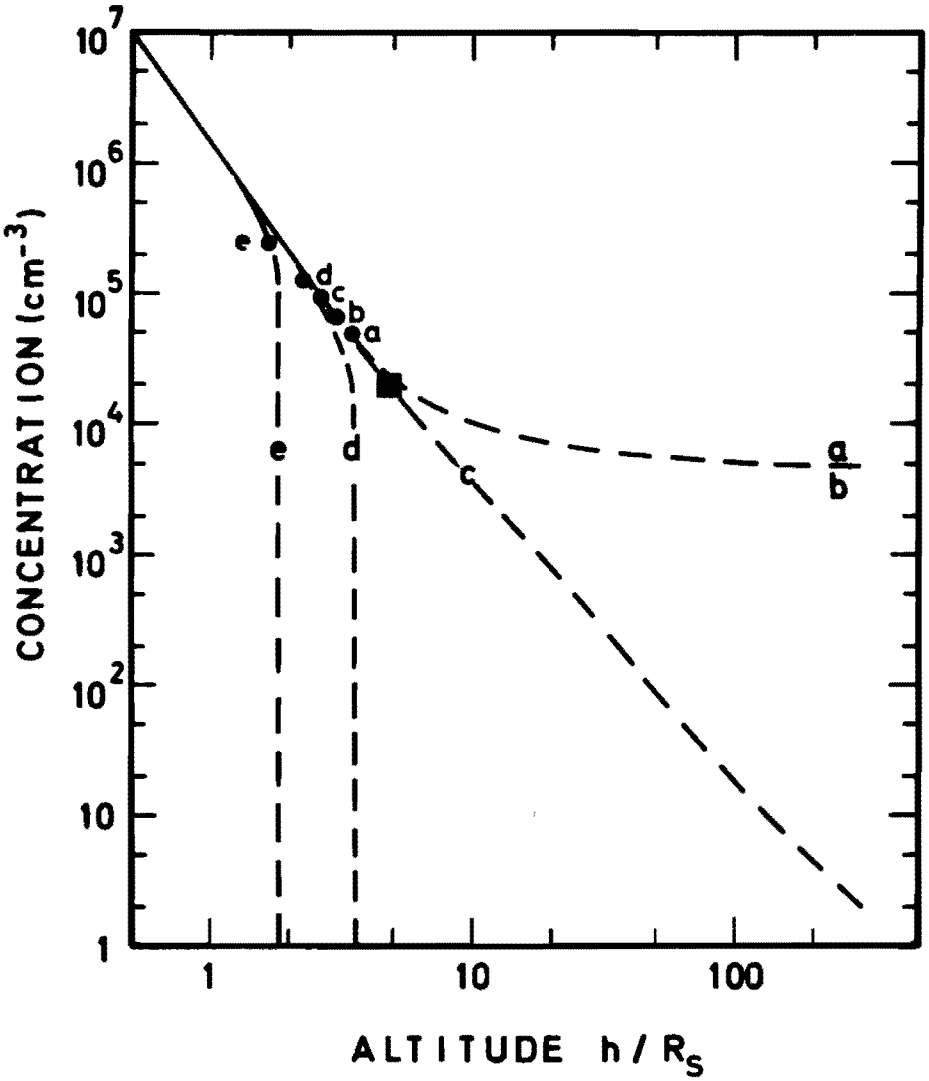

Fig. 4.- Solar wind densities.
The solid and dashed curves refer to hydrodynamic isothermal models for which $T_e = T_p = 10^6$K; at $h_o = 0.5\ R_s$, $n_o = 10^7$ cm^3 and (a) $w_o = 0.8$ km/s; (b) $w_o = 2.15$ km/s; (c) $w_o = (w_o)_c = 3.996$ km/s; (d) $w_o = 4.5$ km/s; (e) $w_o = 7.6$ km/s. The solid dots indicate for each of these five models the exobase altitude (h_{exb}) and density (n_{exb}); the solid square corresponds to the critical point of the hydrodynamic Euler equations.

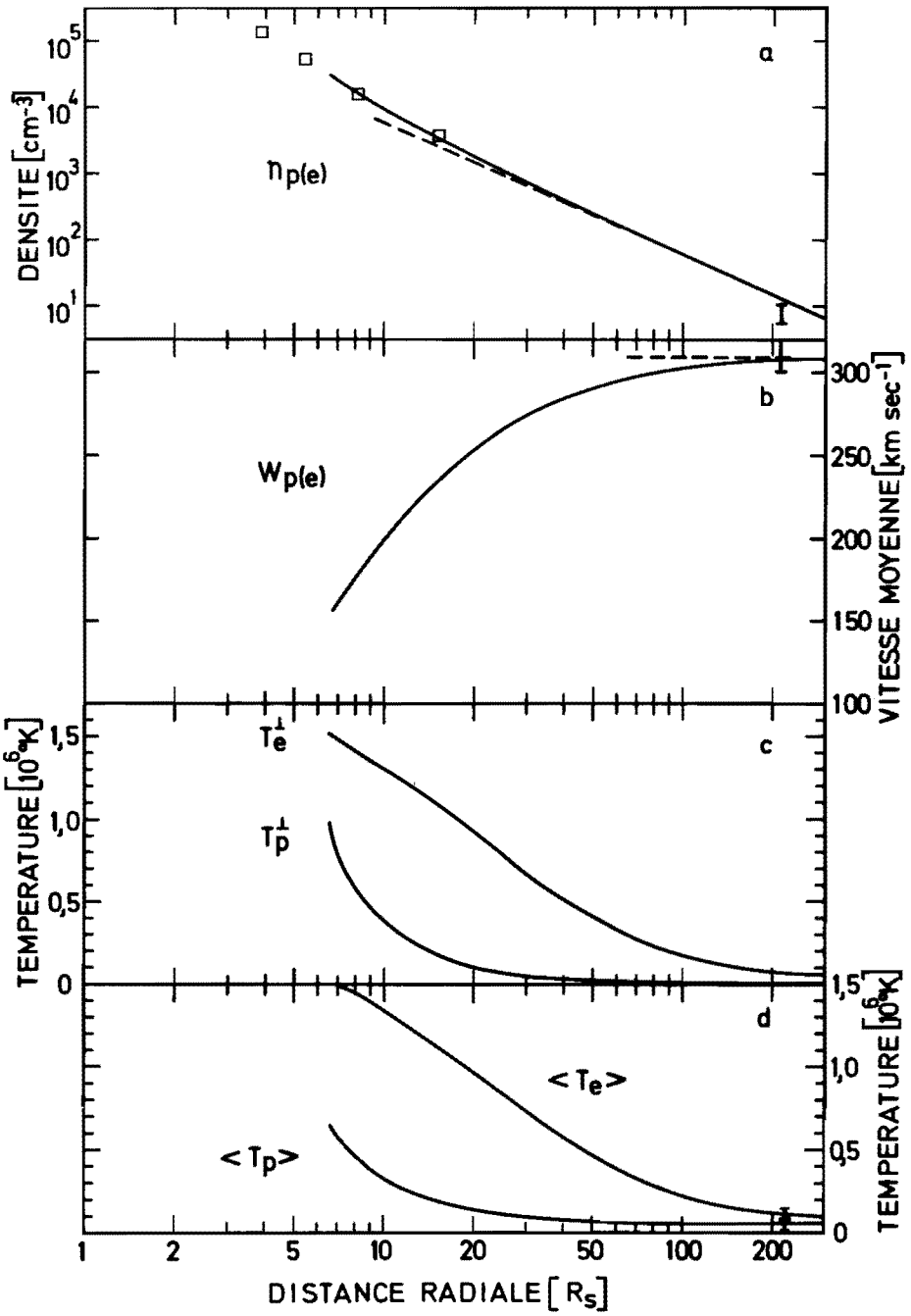

Fig. 5.- The solid lines give (a) the density, (b) bulk velocity, (c) perpendicular temperature, and (d) average temperature of the electrons and protons in Lemaire and Scherer's [1972b] kinetic model 1. The asymptotic behaviors are illustrated by dashed lines. The observed coronal density distribution reported by Pottasch [1960] is shown by squares. The range of observed solar wind properties at 1 AU are taken from Hundhausen *et al.* [1970] and are indicated by vertical bars.

DISCUSSION

Flower :

How is continuity between the inner (fluid model) and outer (kinetic model) regions established ? Are the gradients of the flow parameters continuous ?

Lemaire :

The fitting of hydrodynamic solar wind models (determined for the collision-dominated) and a zero order kinetic solution is made across the exobase by imposing the density, flux of particles, pressure, energy flux ... to be continuous. Because of the assumption that on one side of the exobase the mean free path is small and on the other side it is considered to become infinite (in the zero order kinetic models) the derivatives (gradients) of the density, velocity, heat fluxes ... are not continuous. But in first order kinetic models matching of these gradients might probably be possible.

Benz :

I don't agree with the notion of "protons becoming collisionless at 5 solar radii". Of course, this is true for protons having the mean thermal velocity, but not if they move faster. Then they may become collisionless long before. Since the density decreases about exponentially, the higher density farther down compensates for the smaller ratio of protons with speeds high enough to leave the corona without collisions. My point : the separation of hydrodynamic fluid and kinetic particles must be made in velocity space and not at a certain height.

Lemaire :

The exobase that we have considered is for a thermal proton, where the bulk of the velocity distribution is located. The higher energy particles become of course collisionless even at lower altitudes. Jenssen has taken this into account. It would be useful to reconsider this kinetic model with a selfconsistent charge separation electric field.

Benz :

Furthermore I think it is impossible to accelerate helium ions in your model. They would come up to 5 solar radii and stay there.

Lafon :

I think that the major uncertainty of kinetic models comes from the assumptions concerning the particles trapped in closed orbits, which are independent of boundary conditions. Don't you think that this is an important cause of differences between kinetic and hydrodynamic models ?

Lemaire :

The trapped orbits for the electrons in the zero order kinetic approaches are assumed to be populated and considered in thermal equilibrium with those coming from exobase. This arbitrariness can only be levelled off when some collisional process (Coulomb interactions or wave-particle interactions) is taken into account in the ion-exosphere. But these first order kinetic models have still to be worked out consistently.